

Supporting information for : "Contrasted trends in chlorophyll-a satellite products"

Etienne Pauthenet¹, Elodie Martinez¹, Thomas Gorgues¹, Joana

Roussillon¹⁴, Lucas Drumetz², Ronan Fablet², Mailys Roux¹³

¹IRD, CNRS, Univ. Brest, Ifremer, Laboratoire d'Océanographie Physique et Spatiale (LOPS), IUEM, Plouzané, France.

²IMT Atlantique, UMR CNRS LabSTICC, Technopole Brest Iroise, France.

³École Normale Supérieure, Université Paris Sciences et Lettres, 46 Rue d'Ulm, Paris, France

⁴IRD, Géosciences Environnement Toulouse (GET), UMR5563, CNRS, Université Toulouse 3, 14 Avenue Edouard Belin, 31400

Toulouse, France

Contents of this file

1. Figures S1 to S8

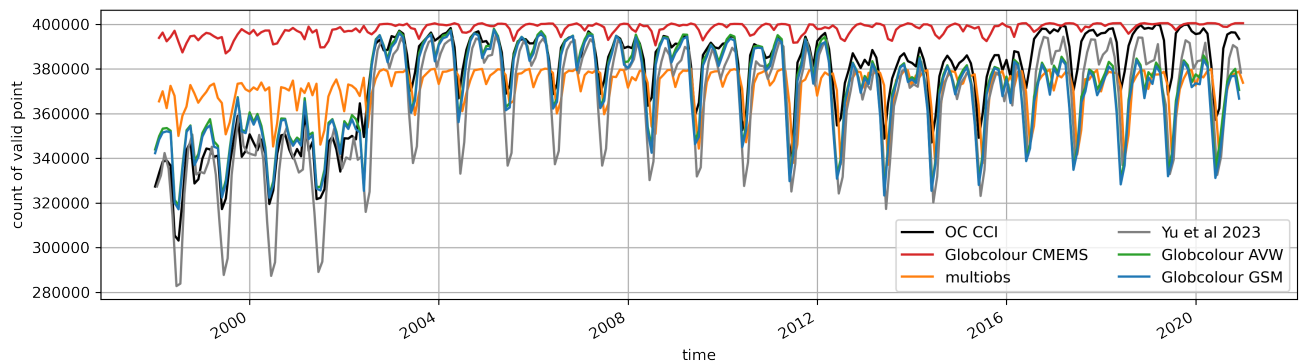


Figure S1. The number of valid Schl data points by month for the six merged products reveals differences that might impact the median presented in figure 2a.

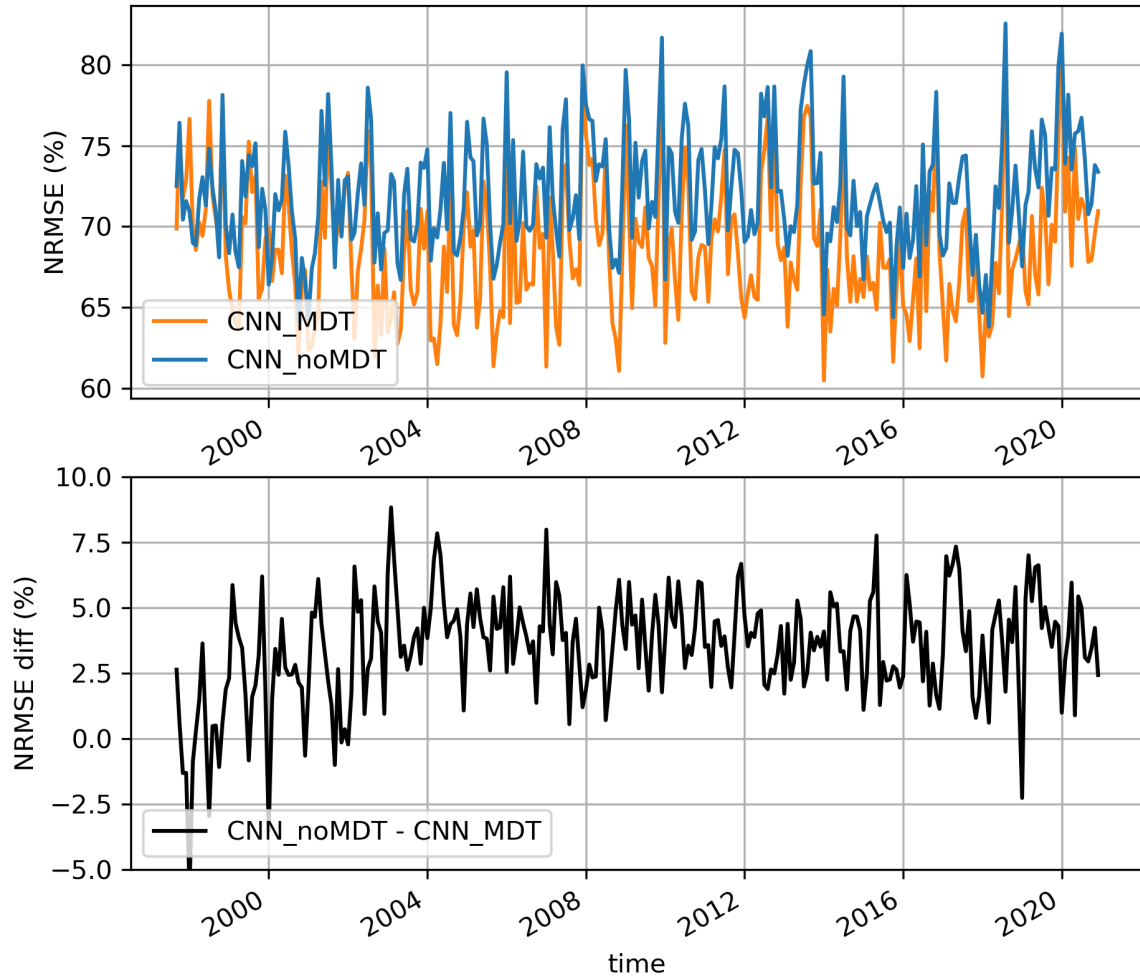


Figure S2. Adding the Mean Dynamic topography to the predictors improves the Normalized RMSE by around 4%. CNN_noMDT is the chl-a trained without MDT in the predictors and CNN_MDT correspond to the architecture as presented in the paper. The difference of NRMSE is displayed on the bottom pannel.

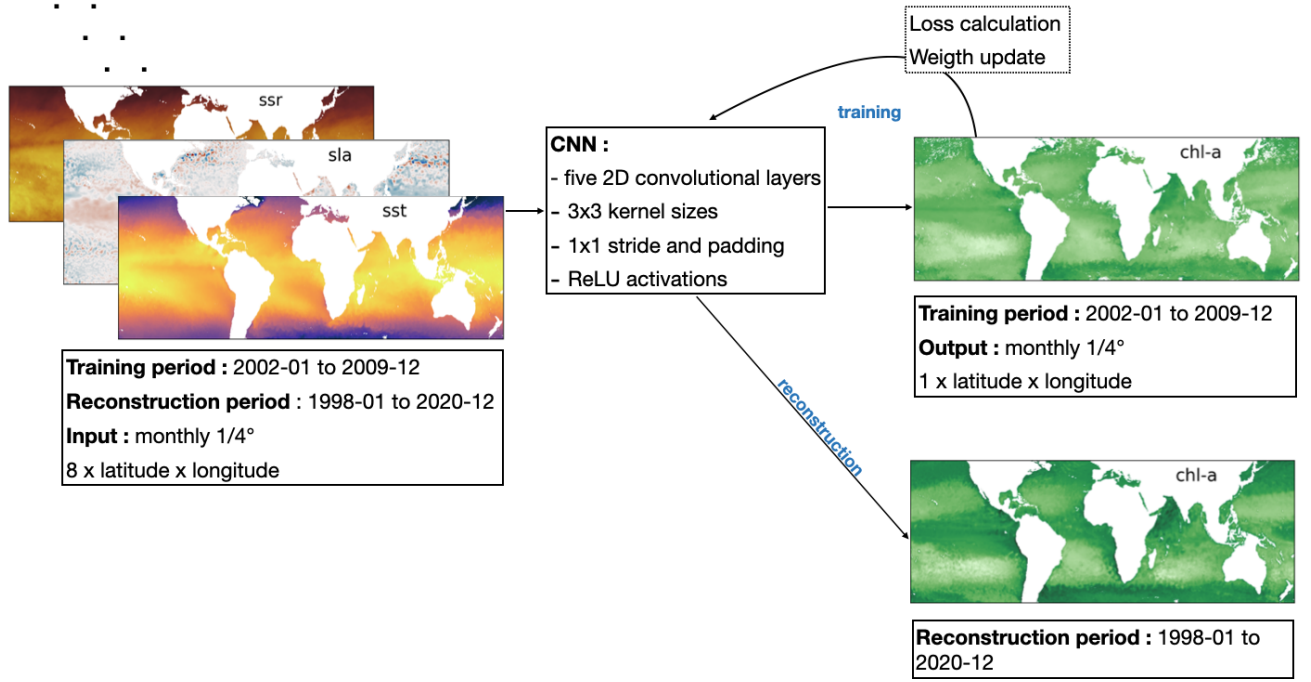


Figure S3. Schematic of the CNN configuration for training and reconstruction of the chl-a from the 8 geophysical predictors (see table 1). For VIIRS, the training and reconstruction period are different (see figure 3 and 4).

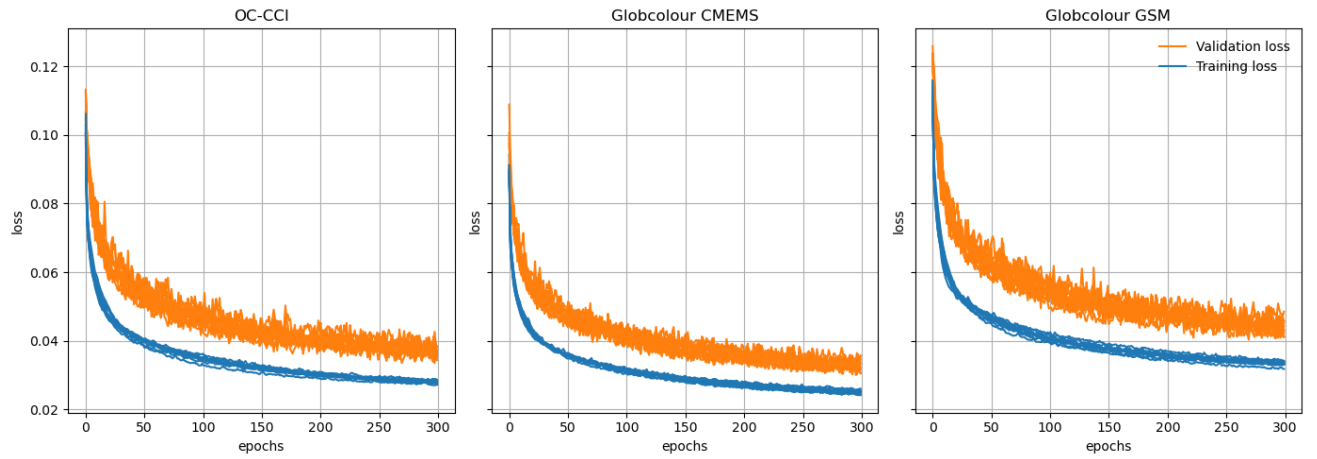


Figure S4. Train and validation loss for the 10 CNNs using OC-CCI, (left), Globcolour CMEMS (middle) and Globcolour GSM (right) as output.

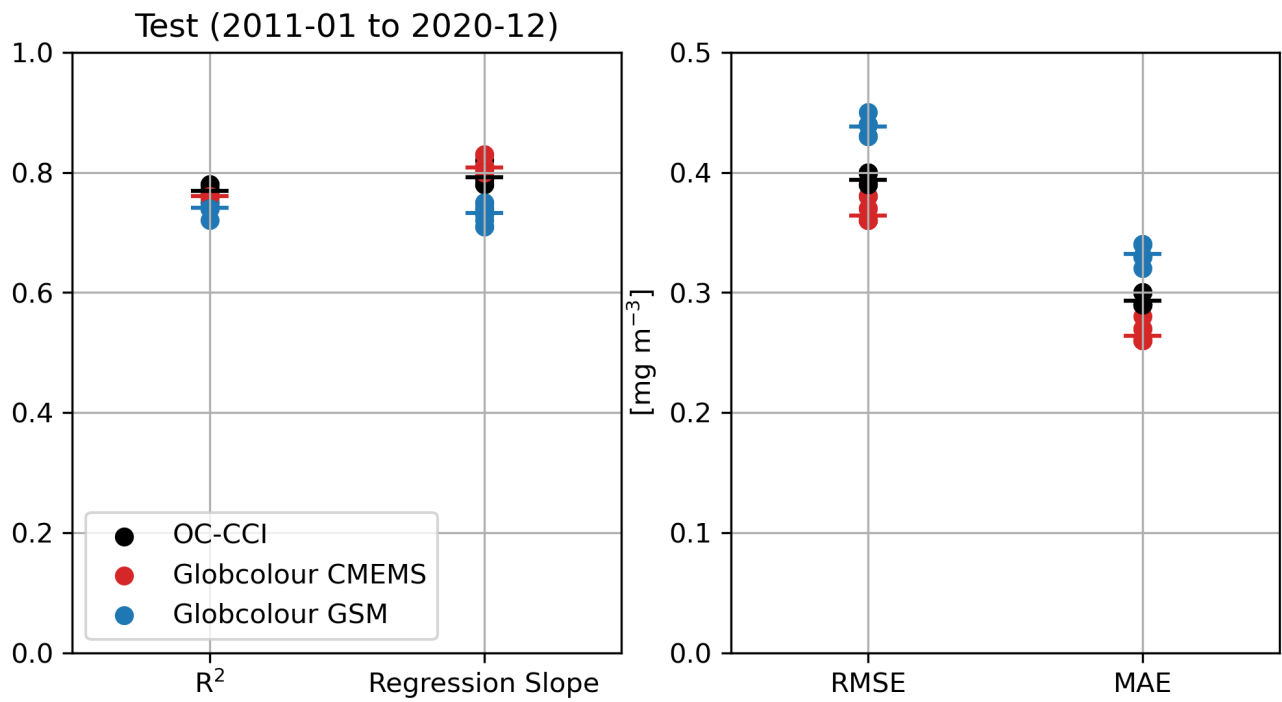


Figure S5. Four metrics to evaluate the test dataset (2011 to 2020) for 10 CNNs prediction for each chlorophyll-a product. The R square and regression slope, and the root mean square error and mean absolute error. The dash line is the mean value of the 10 CNNs.

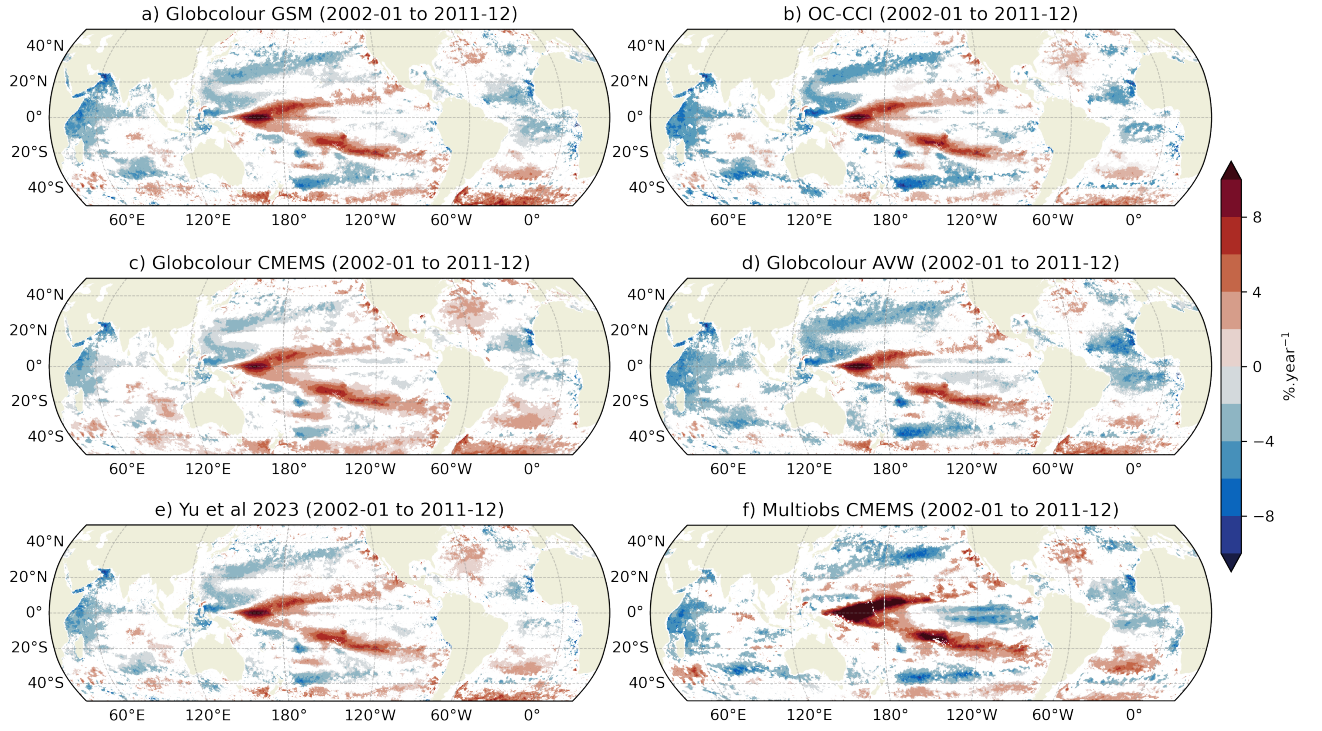


Figure S6. The spatial distribution of the trends of Schl for the period 2002-01 to 2011-12 is consistent between each merged products. The linear trends of the deseasonalised log-transformed surface chlorophyll-a concentration (Schl) is computed for each grid cell and for the region between 50°S and 50°N and the bathymetry deeper than 200m. White areas are indicating non-significant trends ($p\text{-value} > 0.05$).

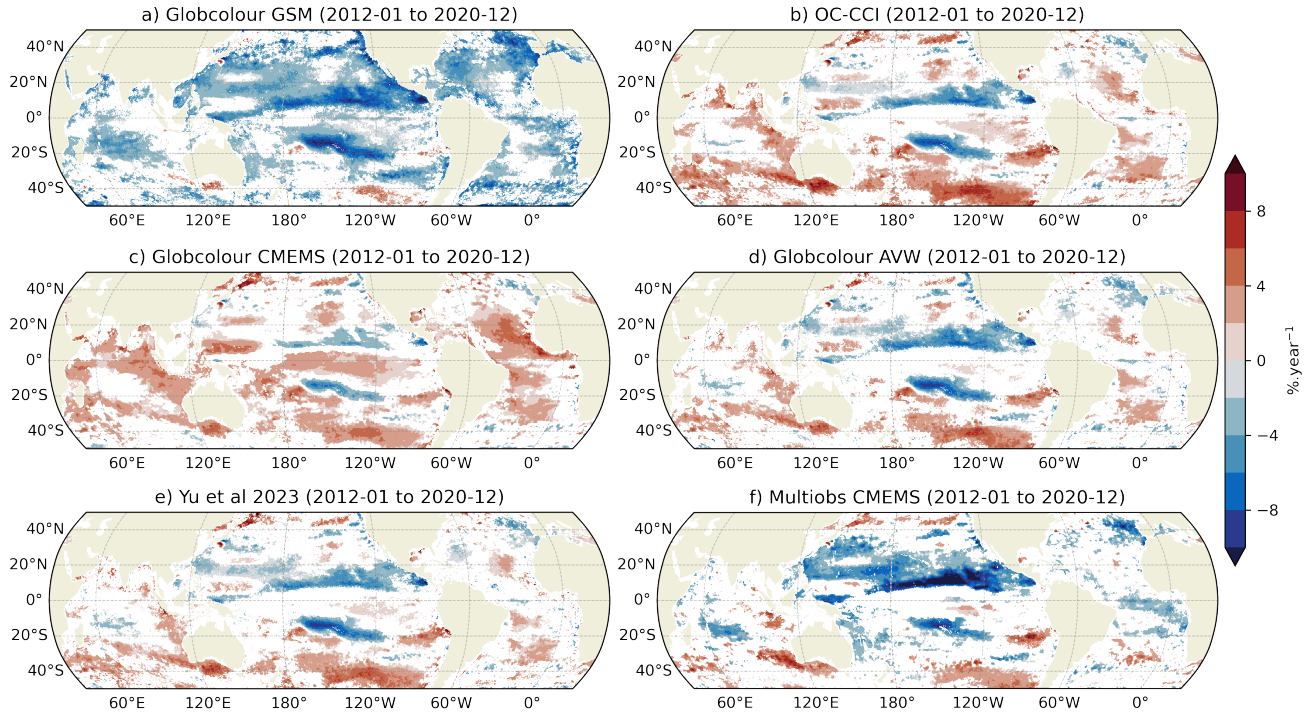


Figure S7. The spatial distributions of the Schl trends for the period 2012-01 to 2020-12 are inconsistent between each merged products. Globcolour GSM differs the most dramatically, with an overall negative trend. The linear trends of the deseasonalised log-transformed Schl is computed for each grid cell and for the region between 50°S and 50°N and the bathymetry deeper than 200m. White areas are indicating non-significant trends ($p\text{-value} > 0.05$). Note that panels a) and b) are also shown on the figure 4a,c.

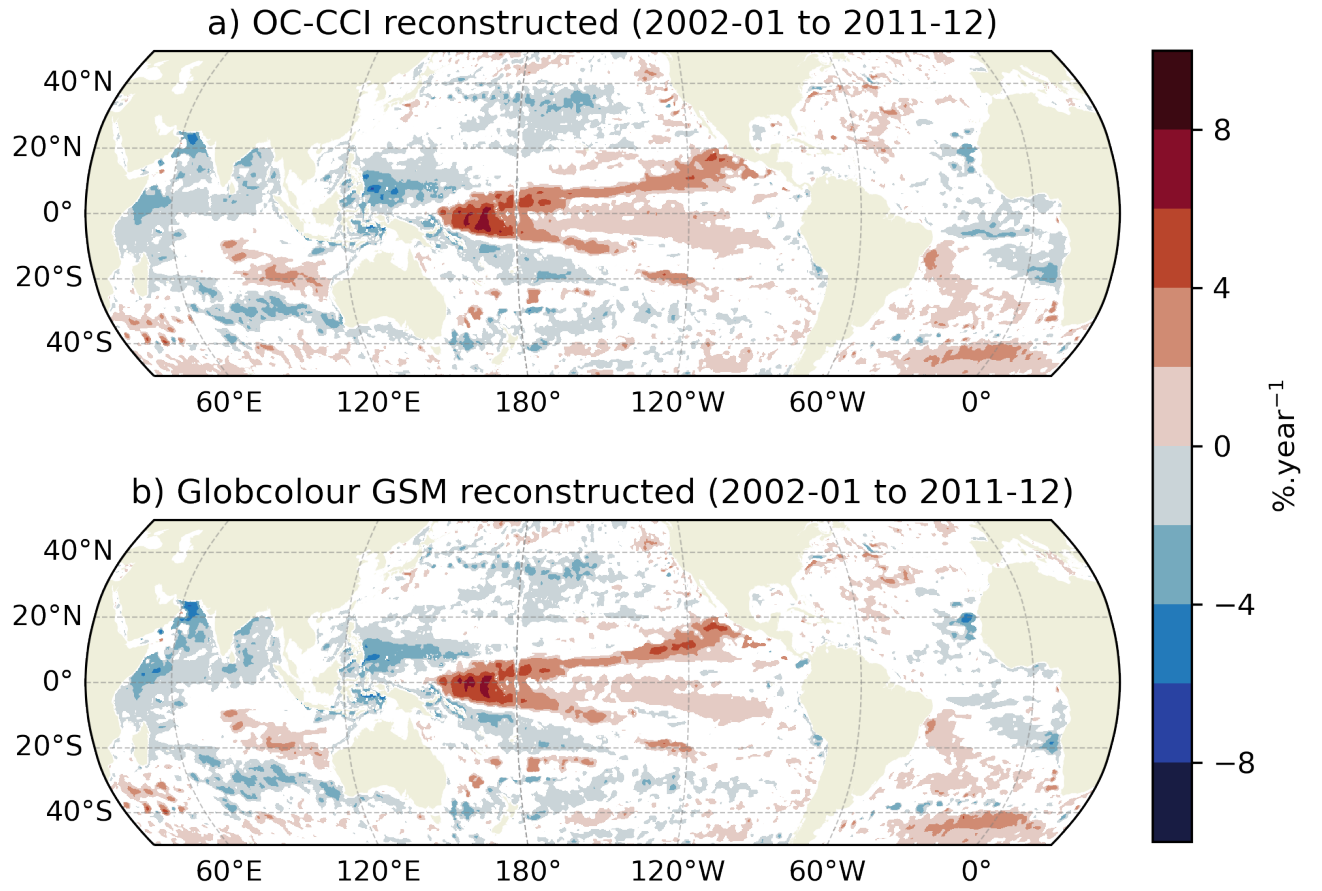


Figure S8. The spatial pattern of the Schl trends over 2002-01 to 2011-12 for the OC-CCI and Globcolour GSM reconstructed by the CNN is similar to the pattern of the observation (Figure S2a,b). The linear trends of the deseasonalised log-transformed Schl is computed for each grid cell and for the region between 50°S and 50°N and the bathymetry deeper than 200m. White areas are indicating non-significant trends ($p\text{-value} > 0.05$).